

# An Efficient Focusing Method for High Resolution Ultrasound Imaging

Kang-Sik Kim

*Department of Bioengineering, University of Illinois at Urbana-Champaign  
(Received October 20, 2005. Accepted January 9, 2006)*

## Abstract

This paper proposes an efficient array beamforming method using spatial matched filtering for ultrasound imaging. In the proposed method, ultrasound waves are transmitted from an array subaperture with fixed transmit focus as in conventional array imaging. At receive, radio frequency (RF) echo signals from each receive channel are passed through a spatial matched filter that is constructed based on the system transmit-receive spatial impulse response. The filtered echo signals are then summed. The filter remaps and spatially registers the acoustic energy from each element so that the pulse-echo impulse response of the summed output is focused with acceptably low side lobes. Analytical beam pattern analysis and simulation results using a linear array show that the proposed spatial filtering method can provide more improved spatial resolution and contrast-to-noise ratio (CNR) compared with conventional dynamic receive focusing (DRF) method by implementing two-way dynamically focused beam pattern throughout the field.

**Key words :** medical ultrasound imaging, spatial matched filter, beamforming, high resolution

## I. INTRODUCTION

Focusing (or beamforming) is one of the most important factors in determining the image quality of ultrasound B-mode images [1-8]. Currently, most ultrasound systems employ different focusing methods at transmit and receive, respectively. First, at transmit, fixed focusing method is used, in which ultrasound waves are transmitted from a subaperture consisting of a number of elements toward a predetermined transmit focal depth. The fixed focusing method provides best spatial/contrast resolution at vicinity of focal depth, but it suffers from degraded resolution at depth which is away from transmit focal depth, near-field and far-field. In other hands, at receive, we can focus the received ultrasound echo signals at every imaging points by selecting appropriate digitized samples received on each channels considering propagation delay time between imaging points and each receive channels, which is commonly called dynamic receive focusing (DRF) [2-7]. And overall B-mode image quality and resolution are affected by both transmit and receive focusing whose performance can be

represented by beam pattern. Therefore, for further improving the resolution of current ultrasound imaging, it is necessary to overcome the limitation of fixed transmit focusing.

To overcome these limitations, current ultrasound systems employ multi-zone transmit focusing, in which ultrasound transmission and reception are performed several times (i.e., 2-8 times) to construct single scanline by changing transmit focal depth per each transmission and reception. However, this method still can not implement perfect or ideal focusing at every imaging depth unlike DRF method at receive, and also suffers from low frame rate in proportion to the number of transmit focal depth.

Therefore, in this paper, efficient focusing method for improving the resolution of ultrasound B-mode image was proposed. In the proposed method, ultrasound waves are transmitted from a subaperture with fixed transmit focus as in conventional array imaging. At receive, each channels construct separate low resolution images, and these low radio frequency (RF) images are passed through spatial matched filters that are constructed based on the system transmit-receive spatial impulse response. And finally the filtered images are then summed. In proposed method, spatial matched filters make it possible to implement dynamic focusing at transmit by overcoming the limitation of fixed transmit focusing. Hence, the proposed method can provide two-way dynamically focused beam pattern, which can be implemented only transmit focal depth in case of current ultrasound system employing DRF, at all imaging point regar-

This work was supported by the Korea Research Foundation Grant.  
(KRF- 2005-214-C00056)

Corresponding Author : Kang-Sik Kim  
Bioengineering Department  
University of Illinois at Urbana-Champaign 3120 DCL,  
MC-278 1304 W. Springfield Ave. Urbana, IL 61801  
Tel : 1-217-390-2353  
E-mail : kangsik@uiuc.edu

dless of location of transmit focal depth. Also, by using matched filter, the proposed method can provide high echo signal-to-noise (eSNR) ratio compared with conventional DRF method. Therefore, the proposed method can improve the overall performance of ultrasound diagnosis including early detection of breast cancer by providing much higher resolution and eSNR compared with DRF method, and can be used as alternative focusing method in case array beamforming is required.

This paper is organized as follows. In Section II, focusing theory is explained using mathematical beam pattern analysis, and based on this basis, the focusing method using spatial matched filter is presented. In Section III, the simulation results using linear array transducer are presented to verify the performance of proposed method. Finally, the paper concludes in Section IV.

## II. METHOD AND ANALYSIS

Fig. 1 represents a two dimensional geometrical model for mathematical lateral beam pattern analysis, where  $x$  and  $z$  represent lateral and axial direction, respectively. In Fig. 1,  $p_1(x_0)$  represents pupil function of aperture, and  $(R_F, 0)$  and  $(x, z)$  represent transmit (or receive) focal point and an arbitrary imaging point in  $x-z$  plane, respectively. Also,  $R_f$  and  $R$  represent distance from a source point  $(x_0, 0)$  on aperture to focal point  $(R_F, 0)$  and imaging point  $(x, z)$ , respectively. Using this geometrical model of Fig. 1 and Rayleigh-Sommerfeld diffraction formula for continuous wave (CW) [8], lateral beam pattern at  $(x, z)$  can be given by

$$\varphi(x) = \frac{1}{j\lambda} \int_{-\infty}^{+\infty} p_f(x_0) \cdot \frac{1}{R} \cdot e^{jkR} \cdot e^{-jk(R_f - R_f)} dx_0 \quad (1)$$

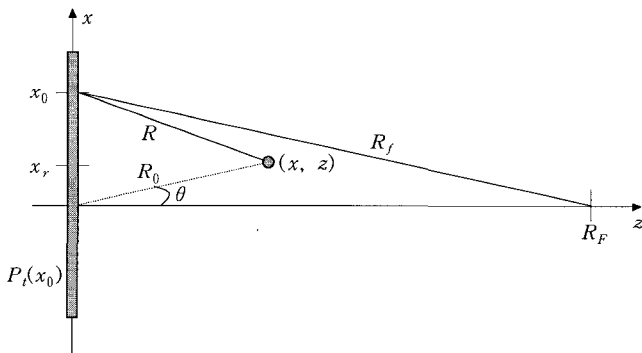


Fig. 1. Model for beam pattern analysis.

where  $k(=2\pi/\lambda)$  and  $\lambda$  represent wave number and wavelength of the used CW signals. And using paraxial approximation [8],  $R$  and  $R_f$  can be expressed by

$$R = \sqrt{(x - x_0)^2 + z^2} \approx R_0 + \frac{x_0^2}{2R_0} - \frac{xx_0}{R_0} \quad (2)$$

$$R_f = \sqrt{x_0^2 + R_F^2} \approx R_F + \frac{x_0^2}{2R_F} \quad (3)$$

where  $R_0 = \sqrt{x^2 + z^2}$  represents distance between origin  $(0, 0)$  to imaging point  $(x, z)$ . Therefore, by substituting (2) and (3) into (1), (1) is expressed by

$$\varphi(x) = \frac{e^{jkR_0}}{j\lambda R_0} \int_{-\infty}^{+\infty} p_1(x_0) \cdot e^{jk\beta x_0^2} \cdot e^{-jk\frac{x}{R_0}x_0} dx_0 \quad (4)$$

where  $\beta$  is defined by

$$\beta = \frac{1}{2R_0} - \frac{1}{2R_F} \quad (5)$$

In manipulating (4),  $1/R$  in (1), representing ultrasound diffraction as wave propagates, is approximated by  $1/R_0$ . Hence, at focal depth, where  $\beta=0$  ( $R_0=R_F$ ), (4) is expressed by

$$\begin{aligned} \varphi(x) \Big|_{R_0=R_F} &= \frac{e^{jkR_0}}{j\lambda R_0} \int_{-\infty}^{+\infty} p_1(x_0) \cdot e^{-jk\frac{x}{R_0}x_0} dx_0 \\ &= c \cdot FT[p_1(x_0)] \Big|_{f_x = \frac{x}{\lambda R_0}} \end{aligned} \quad (6)$$

where  $FT(\cdot)$  and  $f_x$  denote Fourier transform operator and spatial frequency, respectively. And  $c$  represents complex constant term. As shown in (6), lateral beam pattern, when focusing is performed, is given by spatial Fourier transform of aperture. In other words, the role of focusing is to eliminate the quadratic phase term  $\exp(jk\beta x_0^2)$  in (4), which degrades spatial resolution in ultrasound imaging.

In conventional ultrasound system using array transducers, focusing is performed separately at both transmission and reception. Transmit focusing is only performed at single fixed depth while receive focusing can be implemented at every depths by changing receive delay values of each channels, which is called dynamic receive focusing (DRF) method. In DRF method, overall lateral beam pattern,  $\varphi(x)_{DRF}$ , is given by multiplication of fixed transmit beam pattern of (4) and dynamically focused receive beam pattern of (6).

$$\begin{aligned} \varphi(x)_{DRF} &= c^2 \cdot \int_{-\infty}^{+\infty} p_t(x_0) \cdot e^{jk\beta x_0^2} \\ &\quad \cdot e^{-jk\frac{x}{R_0}x_0} dx_0 \cdot FT[p_1(x_0)] \Big|_{f_x = \frac{x}{\lambda R_0}} \end{aligned} \quad (7)$$

Also, lateral beam pattern of DRF at transmit focal depth, which is named DRF-Focus in this paper, can be expressed by

$$\varphi(x)_{DRF-Focus} = c^2 \cdot \left\{ FT[p_1(x_0)] \Big|_{f_x = \frac{x}{\lambda R_0}} \right\}^2 \quad (8)$$

In (7) and (8), the same pupil function  $p_t(x_0)$  was used as both transmit and receive subaperture. Because (8) is the best beam pattern that ultrasound imaging system employing DRF can provide, it can be considered "gold standard" or "ideal beam

pattern.” Therefore, if we can implement the DRF-Focus beam pattern of (8) through all imaging depths regardless of transmit focal depth by overcoming the limitation of fixed transmit focusing, we can significantly improve spatial and contrast resolution of ultrasound image. For achieving these goals, we propose an efficient focusing method using spatial matched filtering (SMF), in which spatial matched filter is used for implementing DRF-Focus through all imaging depths.

Underlying basic idea of the proposed SMF method is to use spatial matched filter instead of delay-sum process for implementing focusing. In other words, if we apply spatial matched filtering to fixed focused beam pattern of (4) along lateral direction, lateral beam pattern can be expressed by

$$\begin{aligned}\varphi(x)_s &= \varphi(x) * \varphi^*(-x) \\ &= c^2 \cdot \int_{-\infty}^{+\infty} \left[ \int_{-\infty}^{+\infty} p_t(x_0) \cdot e^{jk\beta x_0^2} \cdot e^{-jk\frac{\tau}{R_0}x_0} dx_0 \right] \\ &\quad \cdot \left[ \int_{-\infty}^{+\infty} p_r(x_1) \cdot e^{-jk\beta x_1^2} \cdot e^{+jk\frac{(\tau-x)}{R_0}x_1} dx_1 \right] d\tau\end{aligned}\quad (9)$$

where \* and  $\varphi^*(x)$  represent convolution operator and complex conjugate of  $\varphi(x)$ , respectively. By re-arranging the each terms and with the help of Dirac delta function identity, (9) can be expressed by

$$\begin{aligned}\varphi(x)_s &= c^2 \cdot \int_{-\infty}^{+\infty} \int_{-\infty}^{+\infty} \left[ \int_{-\infty}^{+\infty} e^{-jk\frac{\tau}{R_0}(x_0-x_1)} d\tau \right] \\ &\quad \cdot p_t(x_0) \cdot p_r(x_1) \cdot e^{jk\beta(x_0^2-x_1^2)} \\ &\quad \cdot e^{-jk\frac{\tau}{R_0}x_1} dx_0 dx_1 \\ &= c^2 \cdot \int_{-\infty}^{+\infty} \int_{-\infty}^{+\infty} \left[ \delta\left(\frac{x_0-x_1}{\lambda R_0}\right) \right] \cdot p_t(x_0) \\ &\quad \cdot p_r(x_1) \cdot e^{jk\beta(x_0^2-x_1^2)} \cdot e^{-jk\frac{\tau}{R_0}x_1} dx_0 dx_1 \\ &= c^2 \cdot \int_{-\infty}^{+\infty} p_t^2(x_1) \cdot e^{-jk\frac{\tau}{R_0}x_1} dx_1 \\ &= c^2 \cdot FT[p_t^2(x_1)] \Big|_{f_x = \frac{x}{\lambda R_0}}\end{aligned}\quad (10)$$

As shown in (10), output of spatial matched filter for fixed focused beam pattern is equal to the focused beam pattern of (6) except square term in pupil function induced by matched filter. This change in pupil function should be also considered to select optimum apodization window function for various applications. And spatial matched filtering also can be applied to unfocused beam pattern. In this case  $\beta$  can be expressed by  $1/2R_0$  assuming  $R_F$  has infinite value. Therefore, spatial matched filtering can be considered another method for implementing focusing by eliminating the quadratic phase term. Based on this basic idea, SMF method can implement two-way dynamically focused beam pattern, such as DRF-Focusin (8),

at all imaging depths.

We can use the same model in Fig. 1 to explain and analyze the proposed method mathematically. First, in the SMF method, ultrasound waves are transmitted from an array subaperture with fixed transmit focus as in conventional array imaging. At receive, each channels construct separate low resolution images. Therefore, from (4), transmit and receive beam pattern using transmit aperture of  $p_t(x_0)$  and receive aperture  $p_r(x_1) = \delta(x_1 - x_r)$  in Fig. 1 can be expressed by

$$\begin{aligned}\varphi(x; x_r)_{TR} &= c^2 \cdot e^{jk\beta x_r^2} \cdot e^{-jk\frac{x}{R_0}x_r} \\ &\quad \cdot \int_{-\infty}^{+\infty} p_t(x_0) \cdot e^{jk\beta x_0^2} \cdot e^{-jk\frac{x}{R_0}x_0} dx_0\end{aligned}\quad (11)$$

Note that, in (11), fixed focusing and same focal depth are used at both transmit and receive. Therefore, (11) represents the beam pattern of each low resolution images constructed by each single receive channel.

Next, these low resolution radio frequency (RF) images are passed through a spatial matched filter that is constructed based on the system transmit-receive spatial impulse response. Hence, by applying spatial matched filter to (11), filtered signal of each channel can be expressed by

$$\begin{aligned}\varphi(x; x_r)_{TR}^{SMF} &= \varphi(x; x_r)_{TR} * [\varphi^*(-x; x_r)_{TR}] \\ &= c^4 \cdot \int_{-\infty}^{+\infty} \left[ e^{jk\beta x_r^2} \cdot e^{-jk\frac{x}{R_0}x_r} \right. \\ &\quad \cdot \int_{-\infty}^{+\infty} p_t(x_0) \cdot e^{jk\beta x_0^2} \cdot e^{-jk\frac{\tau}{R_0}x_0} dx_0 \left. \right] \\ &\quad \cdot \left[ e^{-jk\beta x_r^2} \cdot e^{+jk\frac{(\tau-x)}{R_0}x_r} \cdot \int_{-\infty}^{+\infty} p_r(x_1) \right. \\ &\quad \cdot e^{+jk\frac{(\tau-x)}{R_0}x_1} dx_1 \left. \right] d\tau\end{aligned}\quad (12)$$

By re-arranging the each terms and using definition of Dirac delta function, (12) can be expressed by

$$\begin{aligned}\varphi(x; x_r)_{TR}^{SMF} &= c^4 \cdot e^{-jk\frac{x}{R_0}x_r} \cdot \int_{-\infty}^{+\infty} \left[ \int_{-\infty}^{+\infty} p_t(x_0) \cdot e^{jk\beta x_0^2} \right. \\ &\quad \cdot e^{-jk\frac{\tau}{R_0}x_0} dx_0 \cdot \int_{-\infty}^{+\infty} p_r(x_1) \cdot e^{-jk\beta x_1^2} \\ &\quad \cdot e^{+jk\frac{(\tau-x)}{R_0}x_1} dx_1 \left. \right] d\tau \\ &= c^4 \cdot e^{-jk\frac{x}{R_0}x_r} \cdot \int_{-\infty}^{+\infty} \left[ \int_{-\infty}^{+\infty} e^{-jk\frac{\tau}{R_0}(x_0-x_1)} p_t(x_0) \right. \\ &\quad \cdot p_r(x_1) \cdot e^{jk\beta(x_0^2-x_1^2)} \cdot e^{-jk\frac{x}{R_0}x_1} dx_0 d\tau \left. \right] dx_1\end{aligned}$$

$$\begin{aligned}
 &= c^4 \cdot e^{-jk \frac{x}{R_0} x_r} \cdot \int_{-\infty}^{+\infty} \left[ \int_{-\infty}^{+\infty} \left[ \delta \left( \frac{x_0 - x_1}{\lambda R_0} \right) \right] \right. \\
 &\quad \cdot p_1(x_0) \cdot p_1(x_1) \cdot e^{jk\beta(x_0^2 - x_1^2)} \cdot e^{-jk \frac{x}{R_0} x_1} dx_0 \Big] dx_1 \\
 &= c^4 \cdot e^{-jk \frac{x}{R_0} x_r} \cdot \int_{-\infty}^{+\infty} \left[ p_1^2(x_1) \cdot e^{-jk \frac{x}{R_0} x_1} \right] dx_1 \\
 &= c^4 \cdot e^{-jk \frac{x}{R_0} x_r} \cdot FT[p_1^2(x_1)] \Big|_{f_x = \frac{x}{\lambda R_0}} \tag{13}
 \end{aligned}$$

As shown in (13), fixed focused transmit beam pattern of (11) before spatial matched filtering is turned into focused beam pattern after the filtering. Therefore, by adding filter output of every channel, final beam pattern can be expressed

$$\begin{aligned}
 \varphi_{SMF}(x) &= \int_{-\infty}^{+\infty} p_r(x_r) \cdot \varphi(x; x_r)_{TR}^{SMF} dx_r \\
 &= c^4 \cdot FT[p_1^2(x_1)] \Big|_{f_x = \frac{x}{\lambda R_0}} \cdot \int_{-\infty}^{+\infty} p_r(x_r) \\
 &\quad \cdot e^{-jk \frac{x}{R_0} x_r} dx_r \\
 &= c^4 \cdot FT[p_1^2(x_1)] \Big|_{f_x = \frac{x}{\lambda R_0}} \\
 &\quad \cdot FT[p_r(x_1)] \Big|_{f_x = \frac{x}{\lambda R_0}} \tag{14}
 \end{aligned}$$

where  $p_r(x_r)$  represents receive aperture. Therefore, proposed SMF method can provide TR-Focus beam pattern of (8) at all imaging depths. For example, if we use linear array transducer of (15) as both transmit and receive aperture, beam pattern of SMF is expressed by (16)

$$p_1(x_1) = p_r(x_1) = \sum_{n=-N}^N \text{rect} \left( \frac{x_1 - nd}{w} \right) \tag{15}$$

$$\varphi_{SMF}(x) = c^4 \cdot \text{sinc}^2 \left( \frac{w}{\lambda R_0} x \right) \cdot \left[ \frac{\sin \left( kd \frac{2N+1}{2R_0} \right)}{\sin \left( kd \frac{1}{2R_0} x \right)} \right]^2 \tag{16}$$

In (15),  $\text{rect}(\cdot)$  and  $2N+1$  represent the rectangular function and the number of active elements, respectively. And  $d$  and  $w$  represent the element width and element pitch, respectively. In (16),  $x/R_0$  terms in  $\text{sinc}(\cdot)$  and  $\sin(\cdot)$  can be represented by  $\sin \theta (= u)$ , where  $\theta$  represents azimuthal angle in Fig. 1. Therefore, (16) can be expressed by

$$\varphi_{SMF}(u) = c^4 \cdot \text{sinc}^2 \left( \frac{w}{\lambda} u \right) \cdot \left[ \frac{\sin \left( kd \frac{2N+1}{2} u \right)}{\sin \left( kd - \frac{1}{2} u \right)} \right]^2 \tag{17}$$

As shown in (17), SMF method provides two-way dynamically focused beam pattern given by  $\text{sinc}^2(\cdot)$  at all imaging depths like multi-element synthetic aperture focusing (M-SAF) techniques [11].

In summary, Fig. 2 represents overall block diagram of proposed SMF method. First, after transmitting and receiving ultrasound wave with fixed focusing, we construct each fixed focused images using each receive channels. And next, apply spatial matched filter to each fixed focused images. At this stage, of course, spatial matched filters are constructed based on the system transmit-receive spatial impulse response. So, after filtering, fixed focused beam pattern is turned into focused beam pattern. Also, relative time delays were also compensated after the filtering. In other words, before the filtering, peak value of each image is located at different position because of different propagation time. However, after

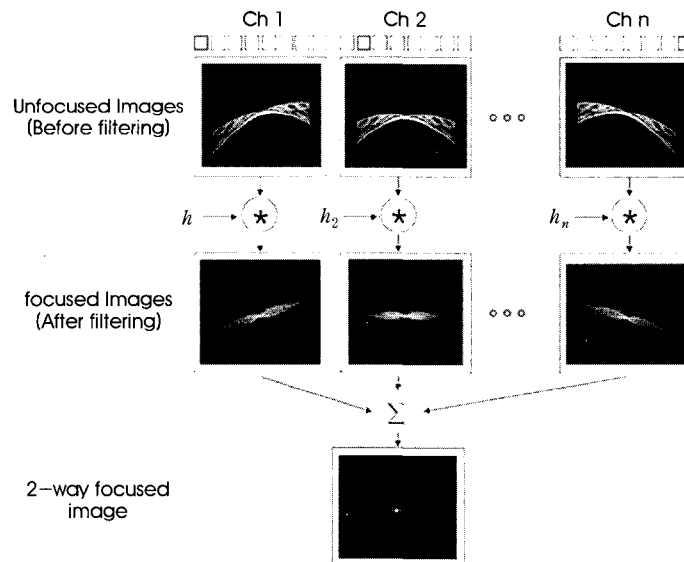


Fig. 2. Block diagram of proposed SMF method.

the filtering, these peak values are located at same position. Finally, by adding all these signals, which have different phase depending on the lateral location of each receive channels, we can construct 2-way dynamically focused beam pattern.

### III. SIMULATION RESULTS

To evaluate the performance of the SMF method, simulations were performed using linear array with center frequency of 10MHz and element pitch of 0.18mm based on Field II [9]. In all simulations, 96 transmit and receive channels were used, and transmit focus is fixed at 40mm for DRF and SMF method. And in case of DRF-Focus, transmit focal depth is set to equal to each imaging depth. Fig. 3 shows continuous wave (CW) azimuthal beam patterns of DRF-Focus, DRF, and SMF method at near-field (20mm), transmit focus (40mm), and far-field (60mm). In Fig. 3, solid line represents DRF-Focus, and dashed line and dotted line represent DRF and SMF method, respectively. As shown in Fig. 3, DRF-Focus method provides beam pattern of  $\sin^2(\cdot)$  at all imaging depths because both transmit and receive focusing is implemented perfectly while DRF provides much more degraded beam pattern at near-field and far field compared with DRF-Focus since transmit beam pattern is degraded except transmit focus in case of DRF.

Also, SMF method shows the almost same beam pattern as ideal DRF-Focus at transmit focus and far-field. In other hands, from (17), theoretical first null location of SMF and DRF-Focus beam patterns in Fig. 3(b),(c) can be calculated by

$$u_0 = \sin^{-1}\left(\frac{\lambda}{(2N+1)d}\right) = 0.51^\circ \quad (18)$$

In Fig. 3(b),(c) measured first null location of SMF is  $0.5^\circ$ , which almost coincides with theoretical value of (18). But, at near-field result of Fig. 3(a), first side lobe level is increased while beam width of SMF is slightly decreased compared with DRF-Focus. These differences from theoretical analysis at near-field is due to the fact that our analysis is based on paraxial approximation of (2) and (3), which doesn't hold good well at near-field. Despite of these differences, however, SMF still provides much improved resolution compared with DRF in term of main lobe width and side lobe level.

Fig. 4 shows point spread function (PSF) of each method. Short pulse having bandwidth of 70% at -6dB were used. And Fig. 5 represents corresponding lateral beam patterns of each PSFs in Fig. 4. In Fig. 5 solid line represents DRF-Focus, and dashed line and dotted line represent DRF and SMF method, respectively. As shown in Fig. 4, at near field, DRF-Focus provides best resolution compared with DRF or SMF method. Unlike the CW beam pattern results of Fig. 3, beam width of

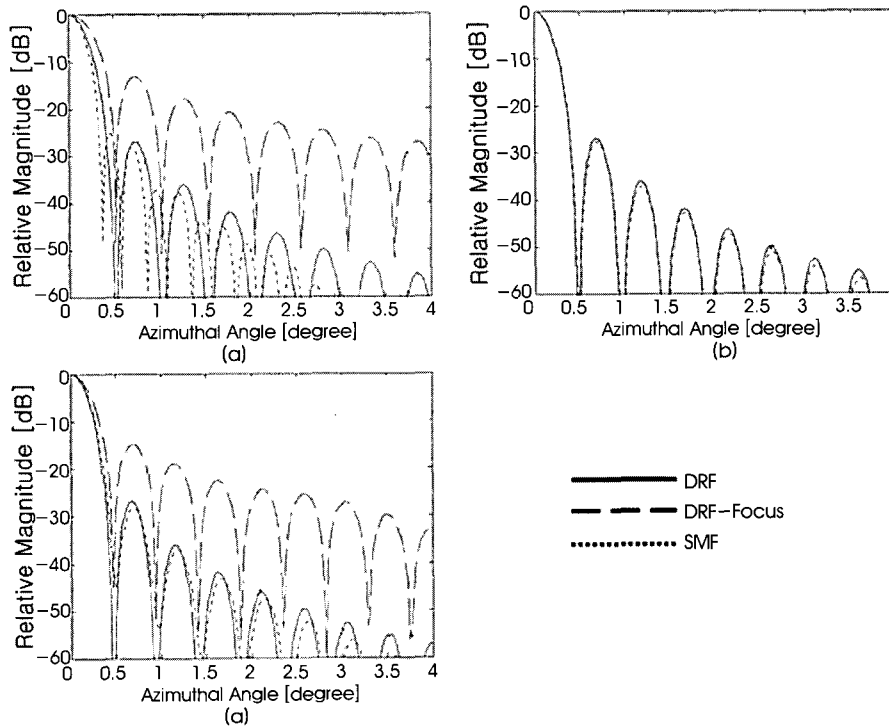


Fig. 3. Comparison of azimuthal beam patterns of DRF-Focus (solid line), DRF (dashed line), and SMF (dotted line) at various depths using continuous wave. Transmit focus is set to 40mm for DRF and SMF. And in case of DRF-Focus, transmit focus is set to each imaging depth. (a) 20mm depth, (b) 40mm depth, (c) 60mm depth

SMF is slightly worse than DRF-Focus. It is because 2-D spatial matched filters were used for constructing 2-D image whereas while 1-D spatial matched filter were used in Fig. 4. However, SMF method provides still much improved resolution than DRF. Also, at transmit focal depth and far-field, SMF

provides almost same resolution compared with DRF-Focus. Especially, at far-field, SMF method shows best resolution. It is because that the 2-D spatial filter remaps and spatially registers the acoustic energy from each element in addition to focusing the beam as shown in Fig. 6 and Fig. 7. Fig. 6(a) and

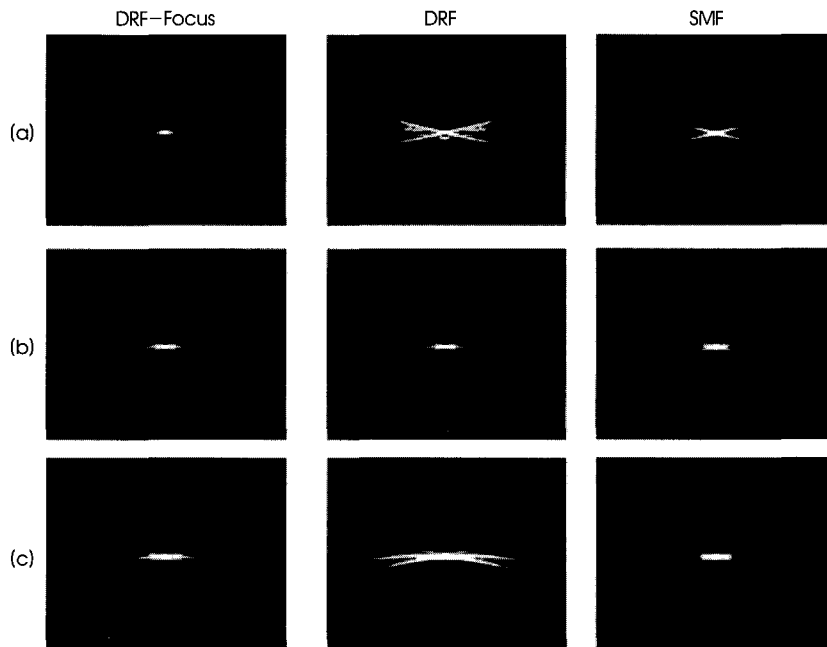


Fig. 4. Comparison of point spread function (PSF) of DRF-Focus, DRF, and SMF at various depths. Transmit focus is set to 40mm for DRF and SMF. And in case of DRF-Focus, transmit focus is set to each imaging depth. (All PSFs are displayed with 60dB dynamic range.)  
 (a) 20mm depth, (b) 40mm depth, (c) 60mm depth

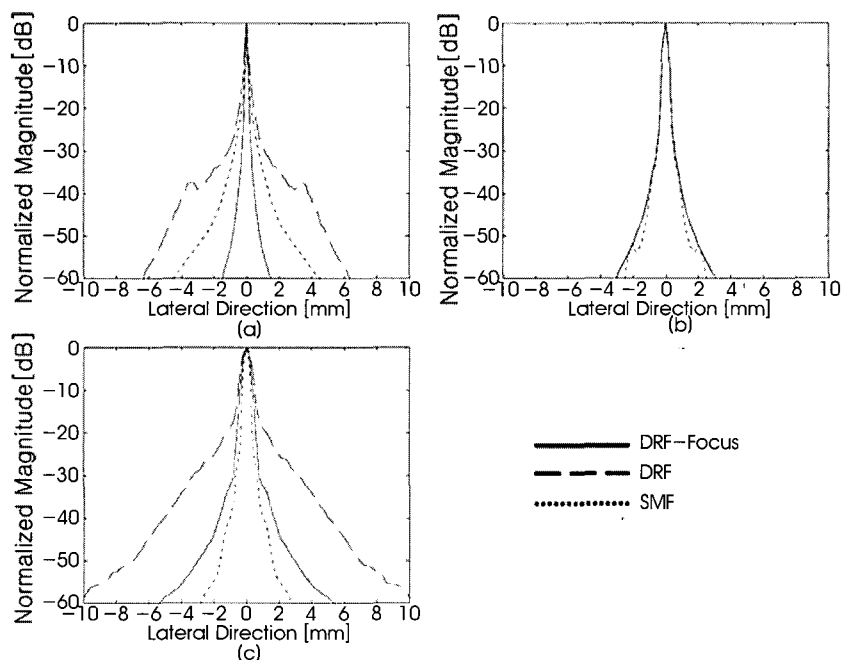


Fig. 5. Comparison of lateral beam patterns of PSF of DRF-Focus, DRF, and SMF in Fig. 4.  
 (a) 20mm depth, (b) 40mm depth, (c) 60mm depth

6(b) represent 2-D beam pattern of center channels before and after the filtering, respectively. Note that in this case, spatial matched filter for Fig. 6(a) is identical with Fig. 6(a), so Fig. 6(b) is 2-D auto-correlation results of Fig. 6(a). And Fig. 6(c) represents 2-D beam pattern of center channel in case of DRF-Focus. Also, Fig. 7 represents corresponding lateral beam patterns of Fig. 6. As shown in Fig. 6 and Fig. 7, beam pattern is turned into focused beam pattern after the filtering. In addition, curved shaped-beam pattern is turned into more linear shaped-beam pattern with slightly lower side lobe level compared with DRF-Focus method. Therefore, SMF method provides best beam pattern at far-field.

In fact, our previous analysis is based on 1-D (or lateral direction) spatial filtering. It doesn't consider 2-D spatial filtering. Due to this limitation, PSF of SMF is slightly different from that of DRF-Focus, especially at near-field and far-field. However, in spite of this difference, SMF method-provides better improved resolution at both near-field and far-field compared with conventional DRF method by providing almost similar beam pattern with DRF-Focus. Especially, at far-field, SMF provides slightly improved resolution compared with DRF-Focus.

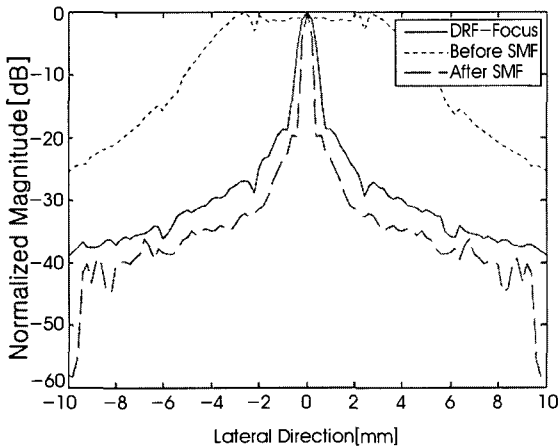


Fig. 7. Comparison of lateral beam patterns of 2-D images in Fig. 6. (Dotted line and dashed line represents beam pattern of Fig. 6(a) and Fig. 6(b), respectively. And solid line represents beam pattern of Fig. 6(c).)

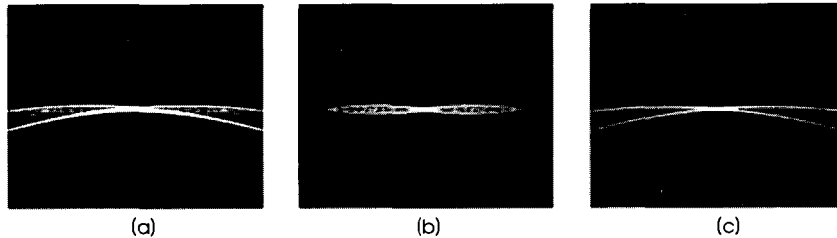


Fig. 6. 2-D images constructed by center channel before the spatial matched filtering (a) and after the spatial filtering (b). Fig. 6(c) represents 2-D images constructed by center channel using DRF-Focus.

Finally, Fig. 8 shows computer generated cyst phantom images constructed using each methods. For SMF method, the same spatial matched filter constructed from each imaging depths (i.e., 20mm, 40mm, and 60mm) were used for filtering the entire images located at different depth. In Fig. 8, all images are displayed with dynamic range of 60dB and each numbers in images represent contrast-to- noise ratio (CNR), which is defined by

$$CNR = \frac{|\langle S_i \rangle - \langle S_o \rangle|}{\sqrt{\sigma_o^2 + \sigma_i^2}} \quad (19)$$

where  $\langle S_i \rangle$  and  $\langle S_o \rangle$  are the mean brightness values inside and outside region of the cyst target, and  $\sigma_i^2$  and  $\sigma_o^2$  are the variances of those regions. As shown in Fig. 8, SMF method provides almost same images with DRF-Focus at 40mm and 60mm. However, at near field, resolution and CNR of SMF image is slightly degraded compared with DRF-Focus like result of PSFs in Fig. 6. But compared with DRF method, image quality and CNR are significantly improved at near-field and far-field.

#### IV. CONCLUSION

An efficient focusing technique using spatial matched filter was proposed, which can provide better lateral resolution than conventional dynamic receive focusing method. It was verified through computer simulations as well as theoretical analysis that proposed SMF method produces ultrasound beams with lateral beam patterns represented as the product of the spatial Fourier transforms of the transmit and receive subaperture. Therefore, SMF method provides two-way dynamically focused beam pattern throughout all imaging points.

In the proposed method, because spatial filters should be applied to each individual channel, system complexity increases due to the 2-D filtering on channel-by-channel. Therefore, efficient filtering algorithms are required which are being investigated by the author.

In addition, in the proposed method, because each unfocused image before filtering can be fully constructed after all transmit

and receive steps are finished, it, such as synthetic aperture imaging techniques [10], requires efficient motion estimation and compensation algorithms to solve motion artifacts problems in case of imaging fast moving object. From these results, we believe that with an efficient spatial impulse response estimation schemes, the proposed method can be used for imaging stationary or slow moving objects with high resolution. Also, the proposed method can be used for implementing focusing in case array beamforming is required.

## REFERENCES

- [1] A. Macovski, Medical Imaging Systems, Prentice Hall, pp.73-224, 1983.
- [2] T. K. Song and S. B. Park, "A new digital array system for dynamic focusing and steering with reduced sampling rate", Ultrason. Imaging, Vol. 12, pp.1-16, 1990.
- [3] M. O'Donnell, et al., "Real-time phased array imaging using digital beam forming and autonomous channel control", IEEE Ultrason. Symp., pp.1499-1502, 1990.
- [4] Zemp RJ, Insana MF, "Spatial coding with curved wave-fronts", IEEE Ultrasonics Symposium, pp.1258-1261, 2004.
- [5] J. Liu, K. Kim, and M. F. Insana, "Beamforming using spatio-temporal filtering", in Proc. IEEE Ultrasonics Symposium, 2005.
- [6] J. A. Jensen and P. Gori, "Spatial filter for focusing ultrasound images," in Proc. IEEE Ultrasonics Symposium, 2001.
- [7] B. D. Steinburg, Principals of aperture and array system design, New York. J Wiley, 1976.
- [8] J. W. Goodman, Introduction to Fourier Optics, McGraw-Hill, 1996.
- [9] J. A. Jensen, "Field: A program for simulating ultrasound systems", Med. Biol. Eng. Comp., Vol. 4, No. Suppl. 1, pt. 1, pp.351-353, 1996.
- [10] K. S. Kim, J. S. Hwang, J. S. Jeong, and T. K. Song, "An Efficient Motion Estimation and Compensation Method for Ultrasound Synthetic Aperture Imaging", Journal of Biomedical Engineering Research, Vol 23, No. 2, 2002.
- [11] M. Karamen, et al., "Synthetic aperture imaging for small scale systems", IEEE, UFFC., Vol. 42, No. 3, 1995.

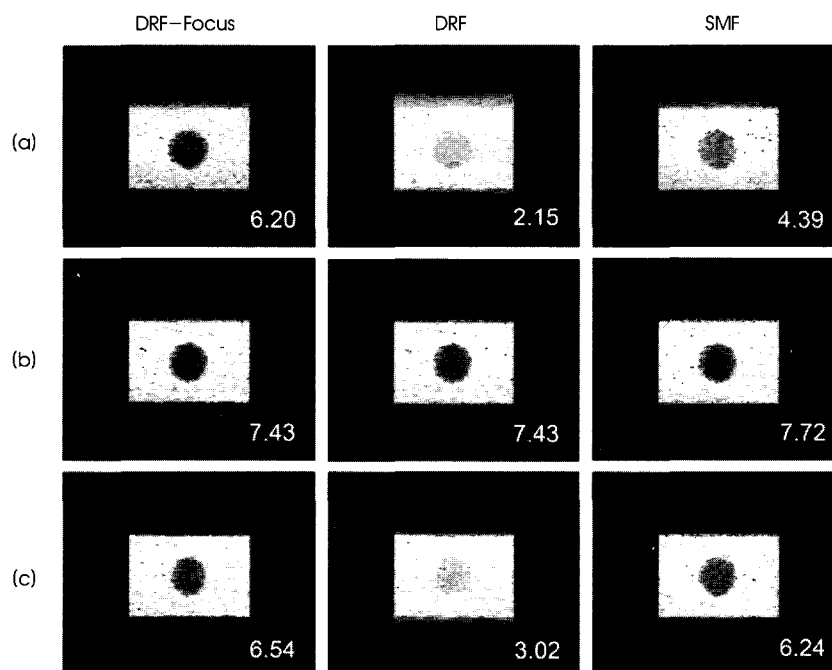


Fig. 8. Simulation results of DRF-Focus (left panel), DRF (center panel), and SMF (right panel) using cyst phantom. Transmit focus is set to 40mm for DRF and SMF. And in case of DRF-Focus, transmit focus is set to each imaging depth. (Diameter of cyst is 4 mm, and its center position is located at  $x=0$ (center of the transducer) and  $z=20, 40, 60$ mm at each depths. Also, CNR is represented at the bottom of each image. And all images are displayed with 60dB dynamic range.)

(a) 20mm depth, (b) 40mm depth, (c) 60mm depth